Constraints on the interior structure and seasonal mass redistribution of Mars from radio tracking of Mars Pathfinder

W. M. Folkner, C. F. Yoder, D. N. Yuan, E. M. Standish, R. A. Preston

Jet Propulsion Laboratory, California Institute of Technology

Doppler and range measurements to the Mars Pathfinder lander, made with its radio communications system, have been combined with similar measurements from the Viking landers to estimate improved values of the precession of Mars' pole of rotation and the variation in Mars' rotation rate. The observed precession of -7600 ± 100 mas/yr limits the range of allowed modeled for Mars interior, placing constraints on the composition and temperature of the mantle. The estimated annual and semiannual rotation variations agree well with a model of seasonal mass exchange of carbon dioxide between the atmosphere and ice caps.

Introduction

The Mars Pathfinder radio system used for communications with the Earth can also be used to measure the distance, and changes in distance, between the Earth and Mars. The Pathfinder signal is usually coherently locked to a signal transmitted by an Earth tracking station. Doppler measurements of the transponder signal are regularly acquired during each communications session. In addition, range measurements have been scheduled once each week. These measurements are being performed to provide determinations of the changing orbits of Earth and Mars and of the rotation of Mars *(1)*. Of particular interest is the Martian rotational information: secular precession and nutation of the spin axis, seasonal and tidal variations in the rotation rate, and Chandler-like wobble of Mars' figure axis relative to the spin axis. These quantities can provide important information on the interior of Mars and on the annual mass exchangebetween the atmosphere and the polar ice caps.

The precession is driven by the gravitational torque of the sun acting on Mars' oblate figure, and is proportional to $(C-(1/2(A+B))/C$ where $C>B>A$ are the principal moments of inertia of Mars. The factor $C-1/2(A+B)=J_2MR^2$ is already known with high accuracy from detection of Mars' gravity field using Viking orbiter and other tracking data (2). Accurate measurement of the precession is needed to determine the polar moment of inertia C. Knowledge of the polar moment of inertia, combined with measurements of the Mars' mass, size, shape, and low order gravity harmonics constrains the range of allowed models for the interior structure.

Mars' rotation rate is expected to vary due to re-distribution of mass by seasonal sublimation and condensation of carbon dioxide at the polar ice caps. Smaller variations are expected due to solar tides. The size of the variations depends on the amount of mass redistribution and on the interior structure.

Previously, radio tracking measurements from the Viking landers have been used to estimate Mars' rotation and orbit (3). From 6 years of ranging to Viking Lander 1, the precession rate was determined to be 7830 ± 300 mas/yr *(4)*. The Viking estimate for the precession constrains the normalized polar moment of inertia, C/MR^2, to be 0.357*0.16. The uncertainty in this estimate is not small enough to distinguish between interior model ranging from an Earth-like composition to iron-enriched compositions characteristic of the SNC meteorites thought to originate from Mars.

We have used the first eight weeks of Pathfinder tracking data to determine the mean spatial orientation of the pole of rotation of Mars to within 2.5". The Viking lander data constrain the mean pole at the midpoint of that experiment to about 0.5". The combination of the Pathfinder data with the Viking lander data acquired 24 years earlier determine the precession rate to about 1.5%, a three-fold improvement over previous results. Improved estimates of the seasonal rotation-rate variations have been achieved by including 2 years of Doppler data from Viking Lander 1 not included in previous analyses *(4)*. Eight weeks of Pathfinder data do not span a large enough fraction of the

Martian to significantly improve the estimates of rotation-rate variations. As Pathfinder tracking data continue to be acquired, they will eventually dominate estimates of rotation variation.

Data quality and estimated quantities

The Pathfinder radio system operates at X-band (8 GHz) compared with the S-band (2 GHz) radio system used by the Viking landers. Because of the higher radio frequency, the Pathfinder data are much less affected than Viking Lander data by fluctuating charged particles in the solar system and in the Earth's ionosphere. The Pathfinder Doppler data have about 13 times less noise. Samples of the Pathfinder data residuals, after removal of geometric and Earth media effects, are shown in Figure 1. The data noise is about 0.05 rends for data at 60 s intervals. Near the end of each Martian day Pathfinder viewed the Earth at low elevation. At low elevation the radio signal traverses a longer distance through the Martian atmosphere. This causes a signature, with amplitude approximately proportional to 1 /sin(elevation), which is visible in the Doppler residuals.

Ranging measurements are also expected to be somewhat more accurate for Pathfinder than for the Viking Landers. The improvement is not as large as for Doppler, partly because the ranging data are more affected by instrumental effects than are Doppler data. Also calibrations for the solar plasma for some of the Viking lander data were determined from dual-frequency observations of the Viking orbiters. The Viking ranging data have a

residual noise of-7 m for data with orbiter calibrations and -12 m for data with no orbiter calibrations. The Pathfinder ranging data taken so far have residuals of-3 rn.

The Doppler and range data obtained during the first 8 weeks of the Pathfinder mission have been combined with data from the Viking landers to solve for Martian orbital and rotational parameters as well as the positions of the Pathfinder and Viking landers. Besides the Viking lander ranging data used in previous work *(4)* we have also included Doppler data from Viking Lander 1 (recovered by Ray Wimberly) from July 1976 to December 1978. The data have been fit using a simplified model for Mars' rotation, with the spin axis direction described by its right ascension α and declination δ *(5)*. Rotation about the spin axis was described the by angle *W*, its rate, ω, and harmonics

$$\delta W = \sum_{j=1}^{4} \{C_j \cos[jn(t - t_0)] + S_j \sin[jn(t - t_0)]\}$$

with t_0 = Jan 1, 1980 and the mean motion n = 190.40°/yr *(6)*. In addition, the solution included six parameters describing Mars' orbit and three parameters (equivalent to the semimajor axis, eccentricity, longitude of perihelion) describing the shape of Earth's orbit. The orientation of Earth's orbit with respect to the frame of extragalactic radio sources used to define Earth orientation was held fixed *(7)*.

Longitude on Mars must be defined by a convention. We have fixed the value for the rotation about the axis, *W*, at epoch J2000, at the value given by Davies et al. *(5)*. Since the estimated rotation rate is different than the value adopted by Davies et al., there is a

cumulative difference in rotation causing a misalignment in longitude at the time of Viking orbiter imaging of about 0.3 km. This is probably less than the camera pointing uncertainties of the Viking orbiter cameras.

Table 1 gives the estimated positions for Pathfinder and Viking Lander 1 & 2. The 'areodetic' coordinates are given with respect to a reference ellipsoid defined by an equatorial radius of 3397.2 km and flatness 0.0105. Table 2 gives the estimated rotation constants. The uncertainties indicated in Table 1 and 2 are not the formal uncertainties, which are much smaller, but account for the unmodeled effects, including polar motion and non-Kelperian corrections to Mars orbit, and encompass variations in solutions observed with subsets of the data and solution parameters.

The right ascension and declination rates of the spin axis are more easily interpreted in terms the obliquity ε and longitude of the ascending node angle ψ relative to Mars orbit normal *(8)*. The estimated obliquity and node rates, after correcting for the periodic nutations *(9)*, are given by

$$d\varepsilon / dt = -20 \pm 50 \; mas / yr$$
$$d\psi / dt = -7597 \pm 100 \; mas / yr$$

where the uncertainties are the realistic uncertainties. The estimated obliquity rate is consistent with zero, as expected. The predicted nodal rate is inversely proportional to the normalized polar moment of inertia C/MR^2, as given by

$$d\psi / dt = -\tfrac{3}{2} J_2 \cos\varepsilon (1-e^2)^{-3/2} MR^2 n^2 / \omega C .$$

where ε is the obliquity and e is the orbital eccentricity. The corresponding moment estimate is

$$C / MR^2 = 0.3653 + 0.0056$$

This represents a threefold improvement over previous estimates *(4)*. The uncertainties in the coefficients describing variations in Mars rotation about its spin axis, $\{ C_j, S_j \}$, given in Table 2 represent a factor of two improvement over earlier results.

Interpretation

Previous estimates of Mars polar moment of inertia required assumptions about the source of triaxial asymmetry of the internal mass distribution. Reasenberg *(10)* used the observed triaxial shape of Mars, and the hypothesis that the Tharsis volcano was the primary contribution to the nonhydrostatic component of the polar moment, to estimate a value for C/MR^2 of 0.365. One means of understanding Reasenberg's argument is to consider the relative magnitude of the nonhydrostatic contributions to the three moments of inertia: $A_C \geq A_B \geq \Delta A$. Tharsis is located near the equator and aligned with the A moment axis. Reasenberg effectively argues that $\Delta C = A_B$. On, the other hand, Bills' *(11)* statistical argument finds that the most likely case is $\Delta C - A_B = A_B - A_A$. The expected moment from this argument is $C/MR^2 = 0.345$. Our estimate clearly favors the Reasenberg interpretation.

The estimated polar moment of inertia can be used to constrain models of the Martian interior. Figure 2 presents the variation in polar moment of inertia versus core size for eight modeled compositions and temperature profiles of the Martian mantle *(4)*. The model mantle composition range from an Earth-like ratio of Mg/(Mg+Fe) of 89°/0 to a value of 70°/0, representing a mantle highly enriched with iron. For each model mantle composition, results for two possible temperature profiles, one cooler than Earth at a given pressure and one warmer, are shown. With no significant constraint on the polar moment of inertia, a wide range of mantle models are consistent with the observed mass, size, and gravitational field. The estimated precession constant rules out some of the models. Warm models with mantles compositions similar to Earth are ruled out, as are some cold, iron enriched models. If the (iron-enriched) SNC meteorites are typical of the mantle composition, then the mantle must be warmer than Earth's (for the same pressure level) and the core radius must be larger than -1300 km. Continued Pathfinder tracking measurements may allow the detection of nutation effects caused by a fluid core *(1)* which would further constrain the size, composition, and temperature of the core.

If Mars has a fluid core with low viscosity (e.g. liquid iron), then variations in rotation about the spin axis depend only on changes in the mantle polar moment of inertia C_m. The major contribution to variations in C_m is the mass exchange between the polar ice caps and the atmosphere. The mass exchange conserves axial angular momentum, and hence the rotation rate changes in response to moment variations. A secondary source of rotation variations is the deformation of Mars' figure by solar tides. Seasonal zonal

winds, which are the primary mechanism for momentum change on Earth *(12)*, are probably much less important for Mars (13).

The unbalanced waxing and waning of the Martian polar ice caps results in seasonal changes in air pressure at the Pathfinder and Viking landers. Assuming that the north and south polar ice caps have uniform thickness and similar angular extent, the predicted change in rotation rate can be inferred from the pressure history *(4)*

$$\delta W(mas) = \overline{K}_{20}\begin{bmatrix} 367\sin(\ell + 112.8°) + 157\sin(2\ell + 181.7°) \\ +19\sin(3\ell + 172.5°) + 8\sin(4\ell + 168.1°) \end{bmatrix}$$

where ℓ is the orbital mean anomaly and $\overline{K}_{20}$ is a factor that depends on several assumptions including the maximurnextent (in latitude) of the ice caps *(14)*. A nominal value is $\overline{K}_{20} \approx 1.3$.

Solar tides result in smaller variations in rotation rate. The predicted response is given by (4)

$$\delta W(mas) = -k_{2m} MR^2 / C_m \begin{bmatrix} 97\sin(\ell) + 62\sin(2\ell + 2\omega - 2\psi) \\ +14\sin(3\ell + 2\omega - 2\psi) + 7\sin(2\ell) \\ -5.9\sin(2\ell + 2\omega - 2\psi) \end{bmatrix}$$

where k_{2m} *is* the mantle tidal Love number. The factor $k_{2m}MR^2/C_m$ ranges from 0.3 to 0.8 for plausible Mars models, with 0.5 taken as a nominal value.

Figures 3 and 4 show comparisons of the predicted ice cap and solar tide models with the estimated values for the annual and semiannual terms. The agreement between the models

and the current estimates for the semiannual term is excellent. The modeled annual term differs from the current estimate by about 100 mas in amplitude and 15° in phase, which is reasonably good agreement given the uncertainties in the model. The quarterly amplitude of 40 mas is just barely significant. However, the triannual amplitude is much larger than predicted. The estimated signature is

$$\delta W_3(mas) = (183 \pm 42)\sin(3\ell + 160.5°)$$

One possible explanation for the observed triannual variation is that there is mass exchangebetween the caps that is not accounted for by the change in pressure. This could lead to a moment change if the caps have different ablation and accumulation histories which vary with latitude *(15)*. For example, one cap may have uniform frost coat while another is maximum at the poles and decreases toward it outer circumference. Or the ice caps might accrete at their outer boundary and ablate uniformly (or vice-versa). Either process could conceivably change the moment without changing air pressure. However, the size of the observed signature implies that this hidden mass is comparable in amplitude to the observed annual signature. Also, it seems odd that the estimated annual and semiannual terms agree so well with the models since this hidden mass effect should also affect them as well.

Another possible explanation for the triannual term is that the signature is not due to rotation-rate variation, but to polar motion, which can cause a signature in the data which is nearly diurnal, mimicking a change in rotation rate. The predicted wobble period

$P_W(day) \cong 191(C_m / 0.365MR^2) / (1 - 0.78k_2)$ ranges from 196 day to 213 day for a wide range of models with a low-viscosity core. This period is close to 1/3 Martian year = 229 day. The estimated amplitude for both the free and forced motions are of order 10 to 20 mas for a 1.5% cap asymmetry. The observed asymmetry of the ice caps during maximum polar winter is quite small, if ice cap thickness is assumed constant, although during summer the residual caps are markedly off-center.

Future improvements

Given the current healthy state of Pathfinder, tracking should continue for many months. Measurements over that time will allow an improved determination of the mean pole during the Pathfinder mission, resulting in improvement of the precession constant. Analysis with a longer span of Pathfinder data and more sophisticated modeling will result in significant improvement in estimates of rotation variations, and should be able to discriminate between possible explanations for the observed triannual signature. There is a good chance that nutation variations due to a fluid core can be detected, which will give much more insight into the structure of the interior, including constraints on the size and composition of the core. The longer tracking arc will also allow improved determinations of Mars' orbit, masses of asteroids affecting Mars' orbit, and tests of general relativity.

Notes and references.

1. W. M. Folkner, R. D. Kahn, R. A. Preston, C. F. Yoder, E. M. Standish, J. G. Williams, C. D. Edwards, R. Hellings, M. Eubanks and B. Bills, J. *Geophys. Res.* **102, 4057 (1997).**

2. A. S. Konopliv and W. L. Sjogren, Publication 95-3, Jet Propulsion Laboratory, California Institute of Technology (1995);

D. E. Smith, F. J. Lerch, R. S. Nerem, M. T. Zuber, G. B. Patel, S. K. Fricke, and F. G. Lemoine, *J. Geophys. Res.* 98,20871 (1995)

3. A. P. Mayo, W. T. Blackshear, R. H. Tolson, W. H. Michael, Jr., G. M. Kelly, J. P. Brenkle, Mysoor and T. A. Komarek, J. *Geophys. Res.* 82,4297 (1977);

W. H. Michael, R. H. Tolson, A. P. Mayo, W. T. Blackshear, G. M. Kelly, D. L. Cain, J. P. Brenkle, I. I. Shapiro, and R. D. Reasenberg, *Science 193,803 (1976);*

E. M. Standish Jr. and J. G. Williams, in *Inertial Coordinate Systems on the Sky,* J. H. Lieske and V. K. Abalkin eds., Kluwer, Dordrecht, pp. 173-181 (1 990);

4. C. F. Yoder and E. M. Standish, J. *Geophys. Res.* **102,4065 (1997).**

5. e.g. M. E. Davies et al., *Celest. Mech.* 63, 127-148 (1996).

6. The estimated terms on variation in rotation about the pole have been corrected for nutations and for general relativistic effects. The effect of nutation on rotation was removed using the approximate correction $\delta W(nut) \approx (\cos\varepsilon - 1)\delta\psi$, where the nutation in longitude of the node, $\delta\psi$, are taken from R. D. Reasenberg and R. W. King, *J. Geophys. Res.* 84, 6231 (1979). The relativistic correction results from the eccentric

Mars orbit and orbital velocity which alters local Mars time by a factor $(1 - GM_O / c2r - \frac{1}{2} V^2 / c^2)$. *See* Ref. 4 and F. W. Sears and R. W. Brehme, *Introduction to the theory of relativity,* Addison-Wesley, Reading Mass. (1968).

7. W. M. Folkner, P. Chariot, M. H. Finger, J. G. Williams, O. J. Severs, X X Newhall and E. M. Standish, Jr., *Astron. Astrophys.* 287,279 (1994)

8. The orbit normal on July 1, 1997 is described by α_o = -86.6416° and δ_o = 65.3206° with respect to Earth Mean Equator at J2000. The unit normal is given by $\mathbf{n}_o$ = $\{\cos\delta_o \cos\alpha_o, \cos\delta_o \sin\alpha_o, \sin\delta_o\}$. The cross product z = $\mathbf{n}_p$ x no defines the line of nodal intersection. The obliquity $\varepsilon = \sin^{-1}(\mathbf{n}_p \times \mathbf{no})$. The rates are obtained from $d\varepsilon/dt = d\mathbf{z}/dt \cdot \mathbf{z}/(\sin\varepsilon\cos\varepsilon)$ and $d\psi/dt = -|d\mathbf{z}/dt \times \mathbf{z}|^2/(\sin^2\varepsilon)$. The explicit expressions are $d\varepsilon/dt$ =0.4146 $d\alpha/dt$ -0.7272 $d\delta/dt$; $d\psi/dt$ = 1.0305 $d\alpha/dt$ + 1.6136 $d\delta/dt$.

9. The periodic nutations shift the nodal longitude ψ during the short Pathfinder epoch by $\delta\psi$ = 1634 mas on Aug. 1, 1997 when the orbital mean anomaly ℓ = -83°. The effect on the Viking data is almost averaged out and is -64 mas on Jan 1, 1980 from numerical partials. The effect on the rate is therefore: $d\psi/dt(nut) = (1634 + 64)$ mas/17.6 yr = 97 mas/yr. A similar correction for obliquity results in $d\varepsilon/dt(nut)$ = 14 mas/yr.

10. R. D. Reasenberg, *J. Geophys. Res.* 82,369 (1977). W. M. Kaula, *Geophys. Res. Lett.* 6, 194 (1979).

11. B. Bills, *Geophys. Res. Lett*. **16,385 (1989).**

12. R. D. Rosen and D. A. Salstein, *J. Geophys. Res.* 88,5451 (1983).

13. A. Cazenave and G. Balmino, *Geophys. Res. Lett.* 8,245 (1981).

14. A harmonic analysis of the Viking pressure measurements gives the size of the seasonal variation coefficients [J. E. Tillman, N. C. Johnson, P. Guttorp, and D. B. Percival, J. *Geophys. Res.* 98, 10963, (1993)]. The rotation response depends on the scale factor $\overline{K}_{20} = (1 + k'_{2m}) MR_e^2 / C_m K_{V1} (K_{20}^{caps} - K_{20}^{P})$. $K_{V1} \cong 0.70$ is the ratio of the average global air pressure to the Viking Lander 1 mean air pressure. The factors K_{20}^{caps} and K_{20}^{P} depend on the angular extent of the ice cap and the topographic effect on global variation of air pressure, respectively. For caps which extend to 55" latitude, $K_{20}^{caps} \cong 0.75$. From a recent topography study (B. G. Bills and R. S. Nerem, *J. Geophys. Res.*. **100,** 26314, 1995), $K_{20}^{P} \cong 0.028$. k'_{2m}, is the mantle load number. For mantles enriched in iron, the ratio $(1 + k'_{2m}) MR^2 / Cm$, *is* near 2,6. For further details, see Ref. 4.

15. As an illustration, consider an ice cap load (mass per unit area) $q(t) = q_o \cos 3nt$ which is uniform over the polar ring from 20° to 35° colatitude. As this mass is transferred to the opposite polar cap, it uniformly ablates/accretes on to a cap with angular radius of 20°, conserving total mass. The resulting change in rotation angle is $\delta W = -0.025(1 + k'_{2m}) MR^2 / C_m (\omega / 3n)(q_o / \bar{\rho} R) \sin 3nt$ where the factor 0.025 comes from the differential cap histories. The required mean surface density within the polar ring to account for a 180 mas triannual signal is $q_o \cong 80 \text{gm} / \text{cm}^2$. This is equivalent to a carbon dioxide ice thickness of about 1 m.

16. We thank the Mars Pathfinder project team for their enthusiasm and assistance in acquiring and understanding the tracking measurements. We thank Ray Wimberly for recovery of the Viking lander Doppler data. The research described in this paper was, in part, carried out by the Jet Propulsion Laboratory, California Institute of Technology, under a contract with the National Aeronautics and Space Administration.

Table 1. Lander coordinates

	Pathfinder	Viking Lander 1	Viking Lander2
Longitude,deg.	W 33.5235±0.0010	W48.2211*O.OO1O	E134.O1O7*O.OO1O
Spherical latitude, deg.	22.2696 *O.OO1O	47.6685 ± 0.0010	19.0952 ± 0.0010
Spherical radius, km	3389.325 ± 0.050	3381.813 ± 0.050	3389.716 ± 0.050
Areodetic latitude, deg.	22.6974+ 0.0010	48.2691 ± 0.0010	19.4726 ± 0.0010
Height from ellipsoid	-2.689 ± 0.050	4.247 ± 0.050	-3.612 ± 0.050

Table 2. Estimated Mars rotation constants

Parameter	Value	Uncertainty
Pole right ascension at J2000, α, deg	317.68113	0.00045
Right ascension rate, deg/century	-0.1070	0.0020
Pole declination at J2000, δ, deg	52.88651	0.00005
Declination rate, deg/century	-0.0608	0.0007
Rotation about pole at J2000, W, deg	176.901	fixed
Rotation rate, deg/day	350.89198233	0.00000015
Annual term C 1, mas	-608	50
Annual term S 1, mas	-96	40
Semiannual term C2, mas	142	35
Semiannual term S2, mas	-220	40
Triannual term C3, mas	-186	40
Triannual term S3, mas	-29	45
Quarterly term C4, mas	38	30
Quarterly term S4, mas	-28	30

mas=milli-arc second of angle

Figure Captions

Figure 1. Typical Doppler data residuals after fit of geometric parameters. The solid line is a fit to the signature due to the Martian atmosphere.

Figure 2. Polar moment of inertia of Mars versus core radius for four different mantle compositions with each of two different temperature profiles.

Figure 3. Comparison of a modeled annual rotation variation from ice cap sublimation/accretion and solar tides with the estimated annual signature.

Figure 4. Comparison ofa modeled semiannual rotation variation from ice cap sublimation/accretion and solar tides with the estimated annual signature.

Fig 1

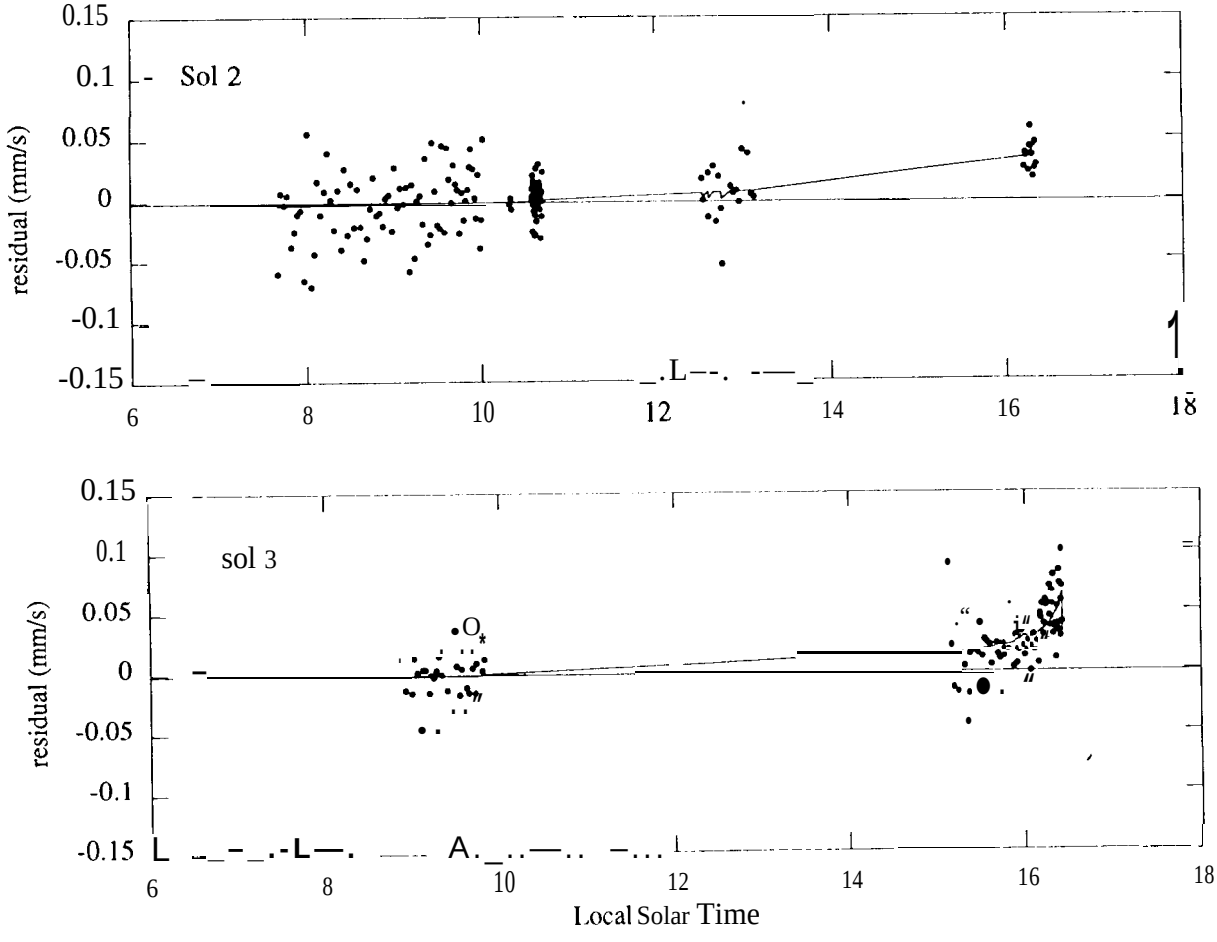
Sol 2
sol 3
residual (mm/s)
0.15
0.1
0.05
0
-0.05
-0.1
-0.15
6
8
10
12
14
16
18
Local Solar Time

Fig 2

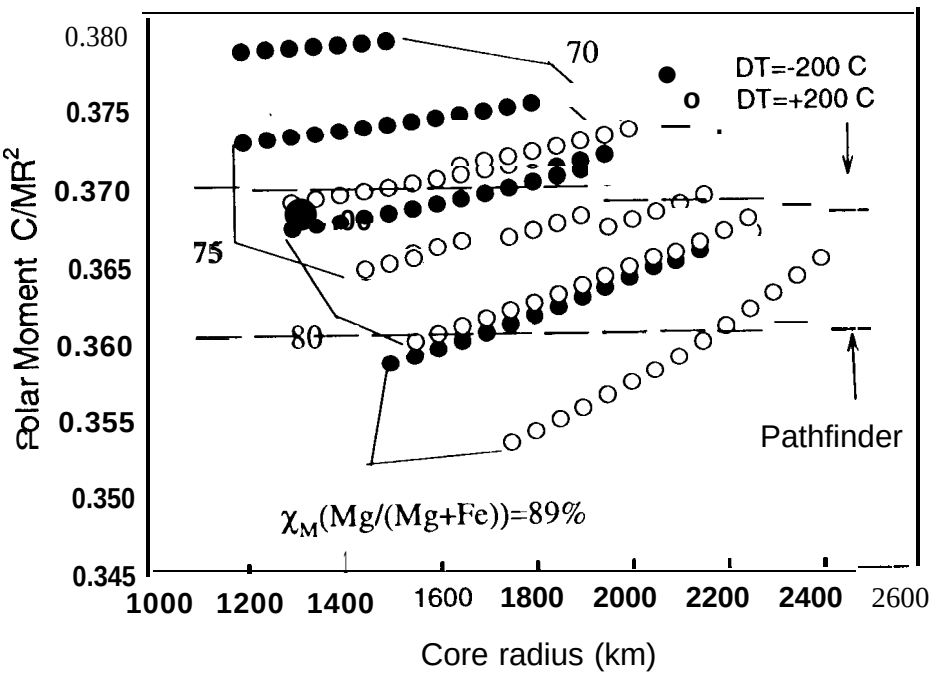
0.380
0.375
0.370
0.365
0.360
0.355
0.350
0.345
Polar Moment C/MR²
70
75
80
DT=-200 C
DT=+200 C
Pathfinder
χM(Mg/(Mg+Fe))=89%
1000
1200
1400
1600
1800
2000
2200
2400
2600
Core radius (km)

Fig 3

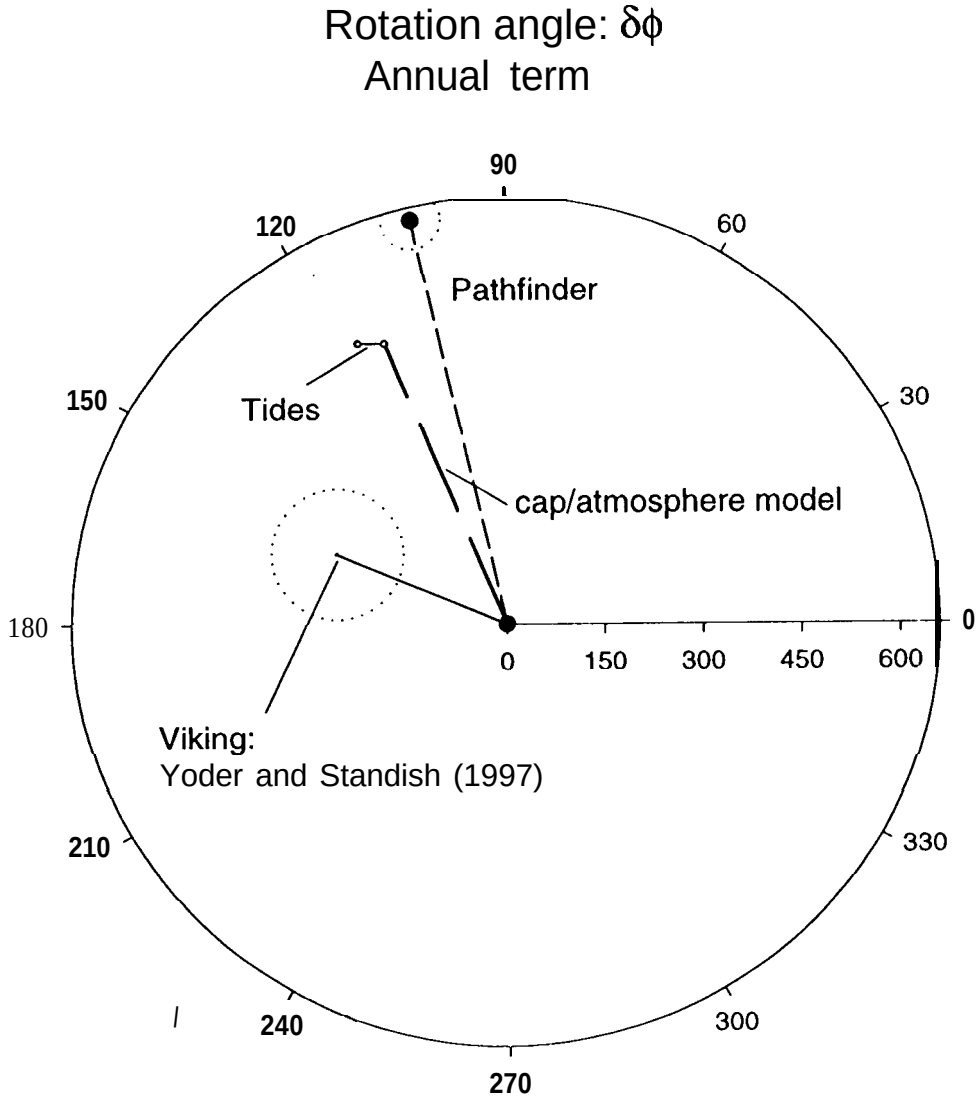
Rotation angle: δϕ
Annual term
90
120
60
150
30
180
0
210
330
240
300
270
0
150
300
450
600
Pathfinder
Tides
cap/atmosphere model
Viking:
Yoder and Standish (1997)

Fig 4

Rotation angle: δϕ
Semiannual term